Techniques for Brain Functional Connectivity Analysis from High Resolution Imaging

A. C. Leitão, A. P. Francisco, R. Abreu, S. Nunes, J. Rodrigues, P. Figueiredo, L. L. Wald, M. Bianciardi and L. M. Silveira

Abstract Several methods have previously been proposed for mapping and enabling the understanding of the brain's organization. A widely used class of such methods consists in reconstructing brain functional connectivity networks from imaging data, such as fMRI data, which is then analysed with appropriate graph theory algorithms. If the imaging datasets are acquired at high resolution, the complexity of the problem both in spatial as well as temporal terms becomes very high. In this work, brain images were acquired using high-field scanners that produce very high resolution fMRI datasets. In order to address the resulting complexity issues, we developed a tool that is able to reconstruct the brain connectivity network from the high resolution images and analyse it in terms of the network's information flowing efficiency and also of the network's organization in functional modules. We were able to see that, although the networks are very complex, there is an apparent underlying organization. The corresponding structure allows the information to flow from one point to another in a very efficient manner. We were also able to see that these networks have a modular structure, which is in accordance with previous findings.

Key words: functional Magnetic Resonance Imaging, brain, network mining, high resolution, graph theory, functional connectivity

A. C. Leitão, A. P. Francisco and L. M. Silveira
INESC-ID/ Instituto Superior Técnico Universidade de Lisboa, Portugal, e-mail: {andrechambel, aplf, lms}@tecnico.ulisboa.pt

R. Abreu, S. Nunes, J. Rodrigues and P. Figueiredo,
ISR/ Instituto Superior Técnico Universidade de Lisboa, Portugal, e-mail: {rodolfo.abreu, sandro.nunes, juliana.rodrigues, patricia.figueiredo}@tecnico.ulisboa.pt

L. L. Wald and M. Bianciardi,
Athinoula A. Martinos Center for Biomedical Imaging, Charlestown, MA USA, e-mail: {wald, martab}@nmr.mgh.harvard.edu

1 Introduction

The human brain is known to be the most complex organ of the human body. Over time its study has attracted considerable attention and researchers have come up with multiple ways to analyse it. One possible way to do that is to build and analyse the brain functional connectivity (BFC) network from the data provided by functional Magnetic Resonance Imaging (fMRI). This BFC network allows to study the brain using standard graph theory algorithms.

This work intends to address this analysis and mapping problem, by starting with high resolution resting state fMRIs obtained from experimental 7T machine scans, extracting from them the BFC network and applying network mining techniques to analyse them. Having a high resolution image of the brain we hope will make it possible to extract a more accurate and more detailed network. However, the increase in data size is also a problem as the amount of data can easily be hundreds of times larger than usual fMRI. Therefore one of the challenges of this work is to find efficient ways to build, represent and analyse these networks.

fMRI

The fMRI is one of the most widely used brain imaging techniques. It relies on the magnetic properties of the hemoglobin measuring the Blood-Oxygen Level-Dependent (BOLD) signal. The brain activity is measured based on the changes in the blood flow and on the fact that the blood flow in the brain is strongly correlated with neuronal activity [1]. The BOLD signal will be more intense in the areas of the brain that are active at a given time. Thus, the fMRI will provide a spatial map of the 3D brain where each volume division (voxel) will have associated to it a different BOLD signal fluctuation. This allows us to know how active that specific volume unit of the brain was through the time course of the test.

Using a stronger magnetic field makes it possible to get higher quality spatial resolution. That property is consequentially reflected on the size and number of voxels, i.e., higher resolution yields more and smaller voxels.

Functional connectivity

The most commonly accepted definition of functional connectivity describes it as the temporal correlation between spatially remote neurophysiological events [2, 3]. In other words the brain functional connectivity network will give us an insight on how the different brain regions are functionally related. Several methods may be used to evaluate functional connectivity. The evaluated functional connectivity may differ depending on whether the complete time series is used or just part of it and also on whether one uses the data from a single subject or the data obtained by averaging across subjects. All these different approaches may yield different functional connectivity networks even though the same datasets are being used. The basic elements of this network will be the voxels the information about voxels functional connectivity will determine if they are connected or not.

Graph theory

To perform all the network mining analysis that are required to obtain the previously described functional network, we resorted to graph theory. A generic graph G consists of a set of nodes, or vertices, (V) connected to each other through a set of edges (E), i.e., G = (V,E). These connections can either exist or not based on the pairwise relation between the nodes.

Often a graph that models the brain functional network can have as vertices the brain's regions of interest (ROI), that are usually known from a brain atlas, which is a three-dimensional map of the human brain. If a more detailed analysis is desired the vertices can be the voxels that come directly from the fMRI.

In graph theory there are several metrics that can be computed for a given graph. In order to understand them there are some baseline concepts that need to be defined first. One simple concept is that of degree of a vertex, which is the number of edges that are connected to it. Another important concept is that of a path, that is the sequence of vertices and edges that are crossed to get from a vertex of the graph to another. The length of a path can be measured by the number of edges that are crossed and this yields the concept of distance between two vertices, as the shortest of all paths that connect them.

2 Methods

In order to analyse the BFC networks using graph theory concepts several metrics were used to give us an insight on the network's structure such as the degree distribution function, clustering coefficient, modularity and small world coefficient, that are defined in [4, 5, 6, 7].

Building a network from fMRI data

In the BFC network each voxel will be a vertex and their pairwise functional connectivity will be an edge. The most commonly used way to determine if there is an edge between two vertices is to measure the correlation between them [8]. Having the correlation between all pairs of voxels a threshold is set and only pairs with a correlation above that level are accepted as functionally connected.

The amount of data that we are dealing with when we compute a matrix that correlates every pair of voxels is a challenging problem, therefore we are going to do some pre-processing before starting the computation. The most obvious step to do first is, on each slice, to only consider the voxels that actually belong to the brain, i.e., voxels that do not have any BOLD signal are no considered. Additionally, we also want to avoid making the computation of the whole correlation matrix at once, an instead do it in chunks. Each of those chunks is then processed to extract the pairs of voxels whose correlation is above the chosen threshold. Those are stored and all other data is discarded. The procedure is as follows: Initially the data matrix

is divided in chunks of equal size where each matrix Y_i has dimensions $m \times t$, with m being the number of voxels and t the number of different time points (Equation 1); Then each of the chunks is correlated with all the other chunks yielding the correlation matrix that is formed by the sub-matrices of the chunks pairwise correlations (Equation 2). All of these sub-matrices will have the same size $m \times m$, m being the number of voxels that are present in each of the data chunks Y_i.

$$Y = \begin{bmatrix} Y_1 & Y_2 & \dots & Y_n \end{bmatrix} \quad (1) \qquad R = \begin{bmatrix} R_{11} & R_{12} & \dots & R_{1n} \\ R_{21} & \ddots & & \\ \vdots & & \ddots & \\ R_{n1} & R_{n2} & \dots & R_{nn} \end{bmatrix} \quad (2)$$

Community detection

We performed a modularity analysis that was intended to find separate modules on the network. The best partition is the one that concentrates more edge density within its modules. The optimization of modularity measure defined by Newman [5] is a hard problem, thus we must rely on efficient greedy algorithms. Even though we are not able to achieve optimal partitionings, we obtain reasonably good ones in linear time. To do so we used a parallel algorithm developed by Boldi et al. [9] called Layered Label Propagation (LLP) that is based on well known label propagation algorithms but with the ability to tune the vertex resistance to change label leading to a hierarchical clustering. The conclusions regarding the different functional modules drawn from these datasets were then compared with a different state of the art analysis. The most commonly used approach to analyse resting state fMRI is the Independent Component Analysis (ICA), and we will therefore be interested in comparing with it. These Independent Components (ICs) can then be compared with our results, to check for their validity. This validation was made by measuring the overlap between the ICs and the modules found by the community detection algorithm. The ICA analysis was conducted using FSL version 5.0.6 with MELODIC version 3.14 [10] generating 20 ICs.

3 Results

The resting-state fMRI datasets were collected from a group of six healthy volunteers on a 7T Siemens machine yielding data with 1.1mm^3 isotropic voxels. As the size of the brain varies from one person to another, each of the subjects has a different number of nodes in their BFC network. These are presented in Table 1.

For each subject, a different correlation threshold yields a different BFC network. This difference can be easily observed when computing the number of edges. The lower the threshold the more voxel pairs are considered as functionally connected thus resulting in a higher number of edges for the lower thresholds.

Subject	Slices	Number of nodes
1	144	1 365 082
2	120	1 080 702
3	133	1 282 836
4	138	1 305 160
5	145	1 365 120
6	135	1 262 244
Average	136	1 276 857

Table 1 Total number of nodes in the BFC network of each subject

	Edge average	Edge density
0.40	668 989 847	8.2067e-04
0.45	302 385 481	3.7095e-04
0.50	136 909 022	1.6795e-04
0.55	61 017 717	7.4852e-05
0.60	26 350 364	3.2325e-05
0.65	10 887 184	1.3356e-05
0.70	4 263 328	5.2300e-06

Table 2 Number of created edges for each subject using different thresholds

As one can observe from Table 2, for all the thresholds the edge density is very low, which makes the network sparse. This was an expected result since in previous state of the art works all the BFC networks were found to be sparse. [11, 7]

Connected components and degree distribution

In order to choose an appropriate threshold it is required to check how much information about the network is lost when going from a low threshold to a higher one. In order to evaluate this, the size of the giant connected component of the network was computed and compared with the total number of nodes in the network. The results regarding these computations are presented in Table 3.

	Subject					
T	1	2	3	4	5	6
0.40	100%	100%	100%	100%	100%	100%
0.45	98%	100%	99%	100%	99%	100%
0.50	77%	100%	91%	100%	88%	99%
0.55	53%	96%	58%	99%	58%	92%
0.60	37%	77%	44%	94%	35%	71%
0.65	26%	48%	32%	74%	23%	55%
0.70	16%	28%	22%	46%	14%	42%

Table 3 Percentage of the total nodes that are in the giant component of the network

From the results presented it is easy to conclude that if the threshold is too high then the network loses its connectivity and the amount of information lost is also too high. We could infer that, on average, for a correlation threshold between 0.4 and 0.5 little information seems to be lost, whereas above that we will start to have is a significant loss of information.

Regarding the vertex degree distribution for the BFC networks it is also dependent on the chosen correlation threshold. To check if our BFC networks exhibit properties similar to the ones already studied in other state of the art works, their degree distribution should follow a power law, with an exponent between 2 and 3. For each subject and for each threshold the degree distribution function was computed and fitted with a power law and the results of the power law exponent that fits each degree distribution function are shown on Table 4.

	Subject					
T	1	2	3	4	5	6
0.40	2.09	2.04	2.15	2.16	2.04	2.28
0.45	2.00	1.92	2.04	2.06	1.97	2.18
0.50	1.92	1.83	1.95	1.95	1.89	2.09
0.55	1.85	1.66	1.86	1.84	1.77	1.96
0.60	1.80	1.64	1.79	1.72	1.77	1.88
0.65	1.77	1.63	1.74	1.66	1.75	1.70
0.70	1.73	1.60	1.66	1.59	1.73	1.65

Table 4 Value of the exponent from the fitting function of the degree distribution

It is possible to see from Table 4 that the networks whose degree distribution is closer to the ones reported in other state of the art works are the ones corresponding to lower thresholds. This is expected as the edge density for the networks with higher correlation thresholds is very low.

Small worldness

Based on the obtained results, the only networks that were considered for further analysis were the ones obtained with a correlation threshold between 0.4 and 0.5.

To prove the small-world topology we need to compute the minimum average path in all the BFC and respective random equivalent networks, and also the clustering coefficient for both cases. With this information we are now able to compute the λ and γ coefficients as presented in [7]. All the results regarding these computations are presented on Table 5 and Table 6.

T	**BFC**	**rand**	λ
0.4	4.113	3.251	1.265
0.45	5.650	3.509	1.610
0.5	7.487	4.698	1.498

Table 5 Average characteristic path for the BFC networks, their respective random equivalents and value of the λ coefficient.

T	**BFC**	**rand**	γ
0.4	0.213	0.053	4.102
0.45	0.197	0.042	4.690
0.5	0.173	0.039	4.436

Table 6 Average clustering coefficient of the BFC networks, their respective random equivalent networks and value of the γ coefficient.

As one can see from Table 5 the minimum average path of all the BFC networks is almost as low as the one from their random equivalents, which is exactly what usually happens in small-world networks [4]. This is an important property of the networks that have a small-world topology, it is possible to go from any vertex to any other with a small number of steps. Regarding the clustering coefficient results, presented in Table 6, we were able to see that these networks have a higher cluster coefficient than its random equivalent. From the previous results it is possible to estimate the σ coefficient, presented in [7] with the results shown in Table 7.

With these final results of the σ coefficient we are now able to postulate that all the studied BFC networks have a small-world topology, since for all of them the σ coefficient is higher than 1, which, as shown in the work of van den Heuvel et al. [7], is enough to prove our assertion of small-worldness.

T	γ	λ	σ
0.4	4.102	1.265	3.243
0.45	4.690	1.610	2.913
0.5	4.436	1.498	2.961

Table 7 Average small-worldness coefficient of all the BFC networks

Community detection

For each of the three different BFC networks of all the subjects a community detection algorithm was applied with the purpose of finding functional modules of the brain. In order to validate these results, the found clusters were compared with the resulting data provided by independent component analysis (ICA).

For the graph cluster analysis only the six major modules were represented because on average the other modules were very small when compared with the average size of the IC. There was some significant overlap between some modules found by LLP and IC found by ICA, with some of these values up to 90%. This is a very relevant result as it proves that our analysis made with the LLP algorithm has very likely found relevant modules of the brain because it is supported by the results of ICA. It was also possible to see that there is a significant overlap of the modules with the ICs in almost every subjects' networks at all three chosen threshold levels; however some thresholds had better results than others. In Figure 1 three modules from the BFC network of subject 3 are represented and also the ICs where those modules are contained. As can be seen, both images are very similar, with the modules that have a higher overlap with the IC being the ones that seem almost the same.

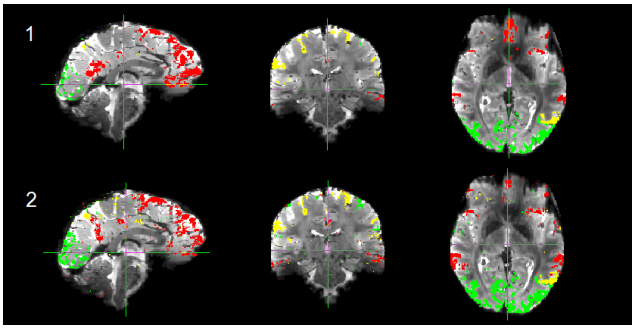

Fig. 1 1 - Three modules found with LLP for subject 3 at a correlation threshold of 0.45; 2 - Three IC found with ICA for subject 3 at a correlation threshold of 0.45

After measuring the overlap between the modules found with LLP and the ICA, we computed their normalized mutual information (NMI). The results showed that almost all the modules and ICs that were chosen have an NMI between 0.3 and 0.5. This may seem an unexpected result because of the high percentage of vertices from the modules that are contained in the ICs. However it is important to stress the fact that the size of the modules sometimes is quite different from the size of the ICs,

which means that although the majority of the vertices from the module overlaps the IC there is still a number of vertices from the IC that is outside of that given module.

4 Conclusions and future work

The results of our work were very interesting, as far as reconstructing the BFC network from high resolution fMRIs is concerned, because to the best of our knowledge no tool has been presented that allows a reconstruction of such high resolution networks. Furthermore, our results also showed that the structural properties of the networks are similar to the ones found in low resolution networks. Thus, even at high resolution, we found that there is an evident ability of the brain's network to flow information in a very efficient way.

Regarding the BFC network analysis, more advanced metrics can be computed and more detailed modularity analysis can be made. For instance, for each cluster that we found another modularity analysis can be performed and checked for clusters within the clusters, i.e., check for some hierarchical information.

It is also important to stress that better and more advanced methods to pre-process the data will yield more interesting and accurate the results. However, all these techniques are also complex specially in datasets that cover areas such as the brainstem, that are very exposed to noise.

Acknowledgements This work was partially supported through FCT, Fundação para a Ciência e Tecnologia, under projects HiFi-MRI, PTDC/EEI-ELC/3246/2012 and PEst-OE/EEI/LA0021/2013, and also by the National Institutes of Health NIH-NIBIB P41EB015896 grant.

References

[1] S.A. Huettel, A.W. Song, G. McCarthy, *Functional magnetic resonance imaging*, vol. 1 (Sinauer Associates Sunderland, 2004)
[2] K.J. Friston, Human brain mapping **2**(1-2), 56 (1994)
[3] B. Horwitz, Neuroimage **19**(2), 466 (2003)
[4] D.J. Watts, S.H. Strogatz, nature **393**(6684), 440 (1998)
[5] M.E. Newman, M. Girvan, Physical review E **69**(2), 026113 (2004)
[6] N.L. Bigg, E.K. Lloyd, R.J. Wilson, *Graph Theory: 1736-1936* (Oxford University Press, 1976)
[7] M.P. van den Heuvel, C.J. Stam, et al., Neuroimage **43**(3), 528 (2008)
[8] S.M. Smith, Neuroimage **62**(2), 1257 (2012)
[9] P. Boldi, M. Rosa, M. Santini, S. Vigna, in *Proceedings of the 20th international conference on World Wide Web* (ACM, 2011), pp. 587–596
[10] C.F. Beckmann, S.M. Smith, Medical Imaging, IEEE Transactions on **23**(2), 137 (2004)
[11] L. Ferrarini, I.M. Veer, et al., Human brain mapping **30**(7), 2220 (2009)